Closed-Form Model for Calculating the Current Induced by the TEM-Cell Center Conductor

Anastasiya A. Drozdova
Department of Television and Control
Tomsk State University of Control Systems and Radioelectronics
Tomsk, Russia
anastasiya.drozdova.00@list.ru

Maxim E. Komnatnov
Department of Television and Control
Tomsk State University of Control Systems and Radioelectronics
Tomsk, Russia
maxmek@mail.ru

***Abstract*— The improvement of the modern electronic component base is aimed at increasing the speed and the degree of integration. This leads to a decrease in the level of immunity of the to external electromagnetic interference. Consequently, it is imperative to analyze the amplitudes and waveforms induced currents and voltages on electronic components at the preliminary design stage. The utilization of analytical models in closed form is more advantageous than numerical methods, as it is less time-consuming. This paper presents an analytical model used to calculate the currents and voltages induced on a microstrip transmission line by the center conductor of a TEM-cell. The effects of sources with different waveforms are shown, namely, electrostatic discharge, the Gaussian pulse and harmonic signals at frequencies of 1 GHz, 100, and 10 MHz. It is shown that the analytical model allows for preliminary estimation of the induced current under the influence of different forms of signals at the TEM-cell input. The adequacy of the proposed analytical model was verified when the printed circuit board thickness and the microstrip transmission line length were varied. The maximum difference between the results obtained by the analytical model and numerical methods does not exceed 25%. A follow-up experiment showed the convergence of the results.**

Keywords—electromagnetic compatibility, magnetic field, transverse electromagnetic (TEM) cell, closed-form equation, microstrip lines

I. INTRODUCTION

Nowadays, radio-electronic equipment (REE) is used in all areas of modern society. The improvement of the modern electronic component base (ECB) used in the development of REE for various purposes is aimed at increasing the speed and the degree of integration, as well as reducing the energy consumption. This leads to a decrease in the level of immunity of the ECB to external electromagnetic interference (EMI). Increasing the level of immunity to EMI is the most critical issue for semiconductor ECD, including integrated circuits (ICs). Measurement of the emission and immunity levels of ICs according to IEC [1], [2] is carried out in a TEM-cell [3]. Using the TEM-cell, it is possible to determine local fault locations in the IC [4] and to estimate the amplitudes and waveforms of currents and voltages induced on the IC. The analysis of amplitudes and waveforms will allow the EMI effects to be simulated and used in the development of new devices and methods of interference protection.

At the preliminary stage of REE design, it is difficult to analyze the currents and voltages induced on ICs without the use of electrodynamic simulation. Therefore, the use of closed-form analytical models at the initial design stage is preferable to numerical methods. To conduct approximate analysis of currents and voltages, simple geometric objects can be used, such as a microstrip transmission line (MSTL). For example, in [5]-[7] the coupling between the MSTL and the TEM-cell is calculated using simple expressions for mutual inductances or capacitances. The analytical model presented in [8] allows estimating the level of interference induced on the MSTL in the TEM-cell. At the same time, this model is demonstrated only for a monopolar pulse, whereas IC tests are performed for harmonic or amplitude modulated pulses. In addition, the resistance of electronic components to electrostatic discharge (ESD) is a critical issue. Therefore, there are different ESD models, such as mechanical (MM) [9], of the charged device (CDM) [10], of the charged printed circuit board (CPCBM) [11] and the charged cable (CCM) [12]-[14].

The aim of this work is to study an analytical model to calculate the currents and voltages induced on the MSTL when different signal sources are fed to the input of the TEM-cell.

II. ANALYTICAL MODEL

The current (I_C) flowing in the center conductor of the TEM-cell creates a magnetic field in the cell. Assuming that the equipment under test (EUT) is located on a PCB (1) with the printed conductors in the form of an MSTL (2), the coupling between the center conductor (3) of the TEM-cell (4) and the MSTL (2), if they are arranged longitudinally, can be represented on the basis of a Gauss theorem for magnetic induction (Fig. 1). The current I_C depends on the voltage standing wave coefficient (VSWR) of the TEM-cell and the voltage applied to its input, as well as on the resistance (Z_C) of the TEM-cell and the matched load (Z_C = 50 Ohm).

The magnetic induction vector flux ($\mathbf{\Phi}_B$) is created by the I_C flowing through the TEM-cell center conductor at a distance of length 2 (a+b) of the circuit in the cross-section of the TEM-cell outer conductor. Moreover, a is the width of the TEM-cell,

---

This work was supported by the Russian Science Foundation Project No. 19-79-10162, https://rscf.ru/project/19-79-10162/

and b is the height. This flux is coupled to the MSTL of length l, located under the center conductor ($\cos(0°) = 1$) at a distance h from the TEM-cell outer conductor.

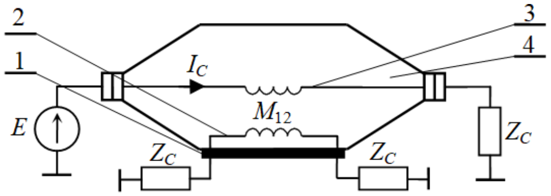

Fig. 1. Magnetic field coupling between the MSTL and the TEM-cell.

The current (I_{EUT}) induced on the EUT can then be determined using the expression from [6]:

$$I_{\text{EUT}} = \frac{\omega \mu_0 I_C l h}{2(a+b)\, Z_C} \text{VSWR}, \tag{1}$$

where ω is the circular frequency and μ_0 is the magnetic constant.

III. ANALYTICAL MODEL VERIFICATION

A. *Waveforms of Excitation Sources*

To verify the analytical model, we chose voltage sources with different pulse parameters, duration (t_d), rise time (t_r) and fall time (t_f) as the influence. The pulse amplitude for all voltage sources was 1 kV. Fig. 2a-d shows the voltage waveforms at the input of the TEM-cell. The ESD voltage waveform by the MM is shown in Fig. 2a, which shows that it has the form of a damped sinusoid with t_r = 10-10.2 ns. The discharge through the CDM is very fast, within 1-2 ns, and t_r = 0.1 ns (Fig. 3b). Fig. 3c shows that the t_d of the charge through the CPCBM is 40-50 ns, and t_r = 2-3 ns. The ESD voltage waveform through the CCM is shown as a rectangular pulse (Fig. 2d) with $t_r = t_f$ = 1 ns and duration t_d = 38-40 ns. A Gaussian pulse (Fig. 3e) with signal rise and fall times $t_r = t_f$ = 0.1 ns and duration t_d = 0.55 ns was chosen as the signal simulating an ultrashort pulse (USP). Harmonic signals at frequencies of 1 GHz (Fig. 3f), 100 (Fig. 3g), and 10 (Fig. 3h) MHz were also used.

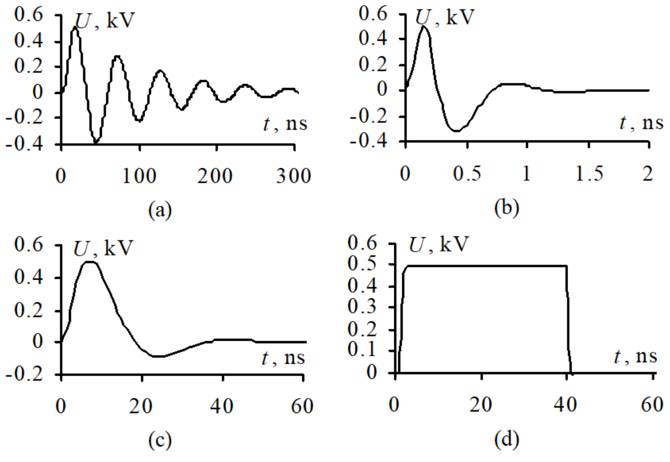

(a) (b)

(c) (d)

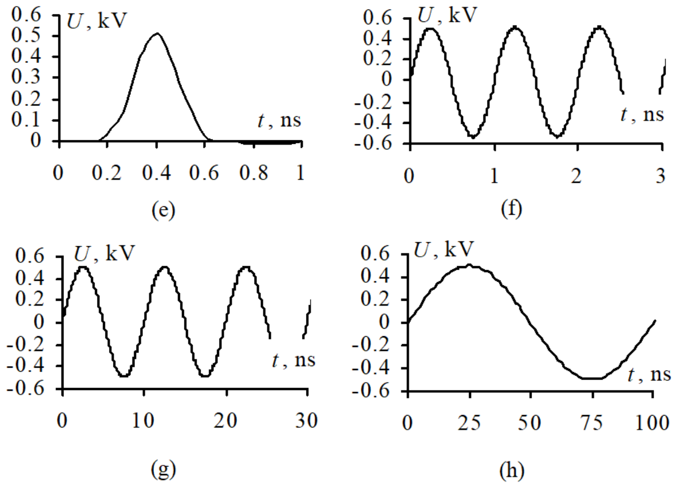

(e) (f)

(g) (h)

Fig. 2. Waveforms at the TEM-cell input when it is exposed to ESD sources by MM (a), CDM (b), CPCDM (c), CCM (d), USP (e), and harmonic signals with frequencies of 1 GHz (f), 100 (g), and 10 (h) MHz.

B. *Calculation of Induced Currents*

To calculate the induced current, we chose an MSTL with the geometrical parameters shown in Fig. 3. The cross-section of this line had the following parameters: the foiled (t_1 = 105 µm) fiberglass with the dielectric permittivity ε_r = 4.3, the thickness h = 0.4 mm. The width of the MSTL active conductor was w_1 = 0.5 mm, the length was l = 70 mm, and the PCB width was a_1 = 100 mm. The characteristic impedance (Z) of this line was 50 Ohm.

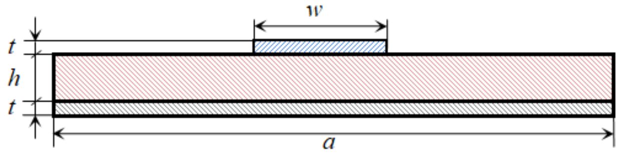

Fig. 3. MSTL cross-section.

The currents induced on the MSTL were calculated using the analytical model (1). In order to validate the results obtained by the analytical method, we carried out software simulations using the Method of Moments (MoM) and the Finite Element Method (FEM). Fig. 4 illustrates the waveforms of the induced currents when the center conductor of the TEM-cell is exposed to different sources.

Fig. 4 shows that the analytical model repeats the waveforms and values of the current amplitudes induced on the MSTL. Table I summarizes the values of the current amplitudes (I_{max}) and their t_r calculated using the analytical model, MoM, and FEM. Table I shows that the I_{max} values calculated using the analytical model are in agreement with the values obtained by MoM and FEM simulations. The maximum difference (δ) in I_{max} values between the analytical model and MoM is 18.8% for the USP (Fig. 4e), while with FEM it is 19.8% for a 100 MHz harmonic signal (Fig. 4g). The minimum δ is 1.9% for the ESD by CPCBM (Fig. 4c) and 1.2% for the ESD by MM (Fig. 4a). The maximum δ of the t_r is 16.7% (ESD by CCM) and the minimum δ is 5.9% (1 GHz harmonic signal).

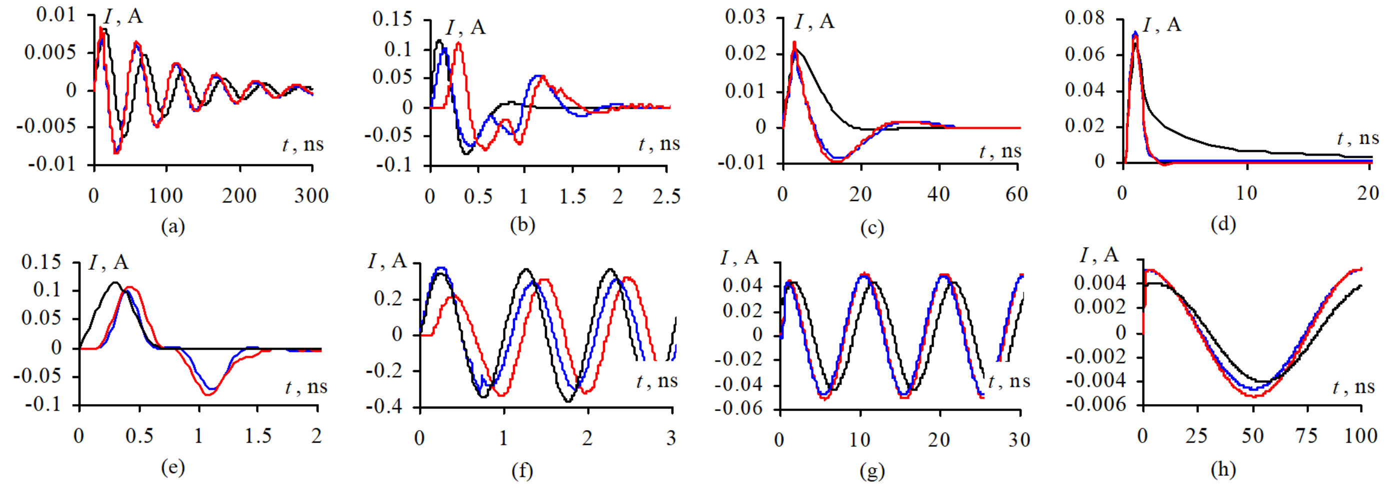

Fig. 4. Current waveforms calculated by the analytical method (–), MoM (–), and FEM (–) when ESD is applied by MM (a), CDM (b), CPCBM (c), CCM (d), USP (e), and harmonic signals with frequencies of 1 GHz (f), 100 (g), and 10 (h) MHz.

TABLE I. CURRENT AMPLITUDES AND RISE TIMES

Impact	I_{max}, mA			t_r, ns		
	Analytical model	*MoM*	*FEM*	*Analytical model*	*MoM*	*FEM*
MM	8.5	7.8	8.4	9	8	8
CDM	115.4	100.8	110.9	0.06	0.07	0.07
CPCBM	21.3	20.9	23.5	2.1	2	1.9
CCM	71.1	75.5	73.4	0.7	0.6	0.6
USP	119.2	100.3	109.3	0.15	0.14	0.16
10 MHz	4.7	5.2	5.3	0.55	0.66	0.65
100 MHz	40.9	48.9	51	0.35	0.38	0.4
1 GHz	322.7	382.7	365	0.16	0.17	0.2

In addition, the induced currents and voltages were calculated when the thickness of the fiberglass (h) and the length (l) of the MSTL were changed. A USP was applied to the input of the TEM-cell. Dependencies of the induced current and voltage at $l = 70$ mm and h varying from 0.2 to 2 mm are shown in Fig. 5a, b and in Fig. 5 c, d – at $h = 0.8$ mm and l varying from 10 to 80 mm.

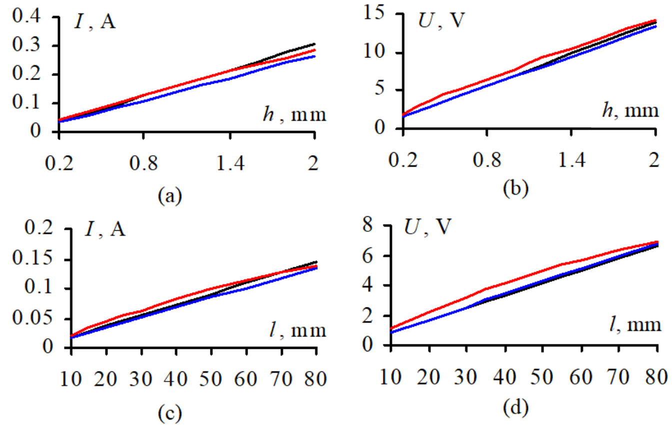

Fig. 5. Dependences of currents (a, c) and voltages (b, d) on h (a, b) and l (c, d) calculated by the analytical method (–), MoM (–), and FEM (–).

From this figure, we can see that currents and voltages induced on the MSTL increase linearly with increasing h and l. Thus, when h is increased from 0.2 to 2 mm, the maximum difference between the results obtained using the analytical model, MoM, and FEM does not exceed 14.8 and 21%, respectively. On the other hand, when l is increased from 10 to 80 mm, this difference does not exceed 7.7 and 24.9%, respectively.

As a result, using the developed analytical model (1), it is possible to calculate the amplitude and waveform of the induced current. Consequently, the currents and voltages induced on the electronic component can be estimated at the preliminary design stage.

IV. EXPERIMENT

To verify the calculation and simulation results, we carried out an experiment. To measure the induced voltage, the experimental setup (Fig. 6b) was assembled according to a schematic diagram in Fig. 6a. The USP voltage was applied to the TEM-cell input [15]. In its aperture, we installed the PCB (1) with the MSTL (2) from Fig. 1 and a solid ground polygon along the edges to ensure electrical contact with the TEM-cell body. A USP generator (5) was connected to the center conductor of the TEM-cell (3), and with a matched load at the end (4). The voltage induced on the MSTL was recorded using a Rohde&Schwarz RTO2044 oscilloscope (6).

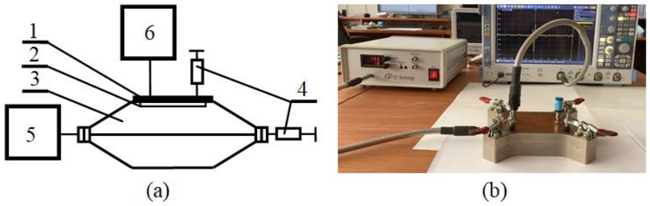

Fig. 6. Schematic diagram (a) and experimental setup (b).

Fig. 7 shows the voltage waveforms measured and calculated using the analytical model (1), MoM, and FEM.

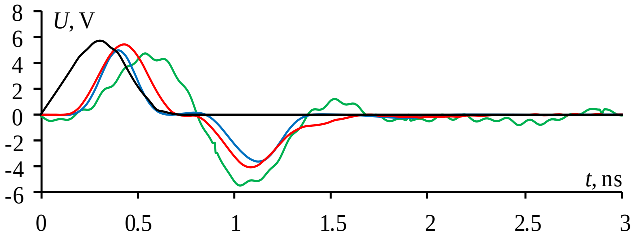

Fig. 7. Voltage waveforms measured (—) and calculated by analytical method (—), MoM (—), and FEM (—).

Fig. 7 shows that the voltage waveforms obtained by calculation, simulation, and measurement are close to each other. For example, the t_r of the signal according to the analytical model was 0.15 ns, MoM – 0.14 ns, FEM – 0.16 ns, and in the measurement it was 0.21 ns. The maximum voltage amplitude was 5.9 V in the analytical calculation, 5.2 V in the MoM calculation, 5.5 V in the FEM calculation, and 4.9 V in the measurement. The insignificant differences between the simulated and measured voltage amplitudes can be attributed to losses in the MSTL conductor and dielectric.

V. CONCLUSION

This paper presents an analytical model to calculate the currents and voltages induced on the EUT placed in a TEM-cell. Different voltage sources were chosen as the impact. We calculated the currents when the center conductor of the TEM-cell was exposed to ESD sources by MM, CDM, CPCBM and CCM, as well as a Gaussian pulse and harmonic signals. It is shown that the analytical model allows performing a preliminary estimation of the induced current under the influence of different signals. The maximum difference between the results obtained using the analytical model and numerical methods does not exceed 19.8%. The adequacy of the proposed analytical model was verified when the thickness of the PCB and the length of the MSTL were varied. It is shown that an increase in thickness and length leads to a linear increase in current and voltage. The maximum difference in values between the analytical model and the numerical methods does not exceed 24.9%. The experiment showed the convergence of all the results.

Consequently, at the initial design stage, the analytical model allows estimating the amplitude and current waveforms when the center conductor of the TEM-cell is exposed to different source signals.

REFERENCES

[1] Integrated Circuits Measurement of Electromagnetic Emissions Part 2: Measurement of Radiated Emissions, TEM Cell and Wideband TEM Cell Method, IEC 61967-2, First Edition, 2005.

[2] Integrated Circuits - Measurement of Electromagnetic Immunity - Part 2: Measurement of Radiated Immunity, TEM Cell and Wideband TEM Cell Method, IEC 62132-2, First Edition, 2010.

[3] M.L. Crawford, “Generation of standard EM fields using TEM transmission cell,” IEEE Trans. Electromagn. Compat., vol. EMC-16, no. 4, pp. 40–46, Nov. 1974.

[4] A.V. Demakov, A.V. Osintsev, V.A. Semenjuk, and M.E. Komnatnov, “Measurement of microcontroller radiated emissions at different operation modes,” 2021 IEEE 22nd International conference of young professionals in electron devices and materials (EDM). Russia, Souzga, pp. 193–197, 2021.

[5] V. Kasturi, S. Deng, T. Hubing, and D. Beetner, “Quantifying electric and magnetic field coupling from integrated circuits with TEM cell measurements,” IEEE Int. Symp. on Electromagn. Compat., Portland, OR, USA, pp. 422–425, 14-18 August 2006.

[6] T. Mandic, R. Gillon, B. Nauwelaers, and A. Baric, “Characterizing the TEM cell electric and magnetic field coupling to PCB transmission lines,” IEEE Trans. Electromagn. Compat., vol. 54, Is. 5, pp. 976–985, Oct. 2012.

[7] S. Deng, T. Hubing, and G. Beetner, “Characterizing the electric field coupling from IC heatsink structures to external cables using TEM cell measurements,” IEEE Trans. Electromagn. Compat., vol. 49, Is. 4, pp. 785–791, Nov. 2007.

[8] A.A. Drozdova and M.E. Komnatnov, “Evaluating the level of electromagnetic interference generated by the ESD source in the TEM-Cell,” 2022 International Siberian Conference on Control and Communications (SIBCON), Russia, Tomsk, pp. 1–7, Nov. 2022.

[9] Electrostatics. Methods for modeling electrostatic phenomena. electrostatic discharge. Mechanical device model. State Standard 53734.3.2-2013 (IEC 61340-3-2:2006). Moscow, Standartov Publ., 2013. 11 p.

[10] Methods for modeling electrostatic phenomena. electrostatic discharge. Charged device model. State Standard 53734.3.3-2016. Moscow, Standartov Publ., 2016. 23 p.

[11] Industry Council on ESD Target Levels. White paper 2: A case for lowering component level CDM ESD specifications and requirements, industry council on ESD target levels. Revision 2.0, 2010. 173 p.

[12] W. Stadler, T. Brodbeck, R. Gaertner, and H. Gossner, “Cable discharges into communication interfaces,” Proceedings of the EOS/ESD Symposium, Tucson, AZ, USA, pp. 144–151, 2006.

[13] K. Chatty, “Model-based guidelines to suppress cable discharge event (CDE) induced latch up in CMOSICs,” IEEE International reliability physics symposium, Phoenix, AZ, USA, pp. 130–134, 2004.

[14] C.J. Brennan et al., “Design automation to suppress cable discharge event (CDE) induced latch up in 90-nm CMOSASICs,” Proceedings of the EOS/ESD Symposium, Anaheim, CA, USA, pp. 126–130, 2005.

[15] A.V. Demakov and M.E. Komnatnov, “TEM cell for testing lowprofile integrated circuits for EMC,” International conference of young specialists on micro/nano-technologies and electron devices (EDM), Russia, Chemal, pp. 154–158, 2020.